Food Research International 43 (2010) 1260–1266

Contents lists available at ScienceDirect

Food Research International

journal homepage: www.elsevier.com/locate/foodres

Prediction of beef meat emulsion quality with apparent light backscatter extinction

D. Álvarez [a,b,*], M. Castillo [a], Y.L. Xiong [b], F.A. Payne [a]

[a] Department of Biosystems and Agricultural Engineering, University of Kentucky, 128 C.E. Barnhart Building, Lexington, KY 40546-0276, USA
[b] Department of Animal and Food Sciences, University of Kentucky, 206 W.P. Garrigus Building, KY 40546-0275, USA

ARTICLE INFO

Article history:
Received 9 October 2009
Accepted 1 March 2010

Keywords:
Meat emulsion
Sensor technology
Fiber optic
Light extinction
Prediction models

ABSTRACT

Normalized light backscatter intensity (I_N) response as a function of fat/lean ratio (R_{FL}; 0.075, 0.25, and 0.33), chopping time (CT; 2, 5 and 8 min) and fiber separation distances (d; 2, 2.5 and 3 mm), were measured using a fiber optic spectrometer. Models based on the apparent light extinction coefficient (model I), fat/nonfat solid concentrations (model II), and the intensity ratio between optical distances (model III), were tested for I_{N_0} prediction (I_N at $d = 0$). Model I was significantly ($P < 0.0001$) better than model II for prediction at 570 nm (λ), 8 min (CT), and 0.075 of R_{FL}. Model III showed maximum geometry values and extinction coefficients for optical fiber separations of 2 and 2.5 mm, yielding the higher R^2 as R_{FL} and wavelength increased. The results demonstrated a high correlation between functional properties of meat emulsion (i.e., R_{FL}) and optical wavebands that may have potential for predicting I_{N_0} using an optic sensor technology.

1. Introduction

Improving meat emulsion control during manufacturing may require the development of an on-line optical backscatter sensor technology for monitoring and controlling emulsification of comminuted meat products during the chopping process. This would allow selection of the optimum level of emulsification to maximize cooking yield and quality or consistency of the final product. The motivation for this topic is the significant economical impact of emulsion breakdown in the meat industry and the non-existence of any effective on-line technology for controlling emulsion stability. The importance of meat quality sensors in the development of the meat-processing industry has been mainly reported in the last two decades (Krol, van Roon, & Houben, 1988). Several fiber optical technologies based on infrared spectrophotometry have been widely used for the analysis of food systems to evaluate different sources of paleness in meat (Swatland, 1982, 1983), to monitor and control the functional properties of comminuted meat batters used in meat processing (Norris, 1984; Swatland & Barbut, 1990), as well as to determine chemical composition of raw beef/pork meat emulsions (Lanza, 1983).

An interesting application of light backscatter sensor technology has been proposed recently by Álvarez, Castillo, Payne, and Xiong (2009). The authors designed, built and tested this optical sensor prototype to measure light backscatter of comminuted meats at different optical probe distances, through which they identified and detected different physical–chemical changes occurring during chopping that were correlated to emulsion stability. Successful development of this unique on-line sensor technology to control meat emulsion stability would have a great impact on industry worldwide in terms of processing efficiency and product quality. However, the appropriate development of this optical sensor technology requires of a clear understanding of the chemical composition and optical heterogeneity of the meat emulsion matrix. This knowledge would aid in the development of a sensor technology capable of accurately measuring different concentrations and sizes of fat particles in meat matrixes so as to effectively detect quality changes during meat emulsification.

Comminuted meat products are a finely chopped, heterogeneous structures composed of water, fat, protein, salt and different amounts of non-meat ingredients. Although every constituent plays at least a minor role in the scattering of light, fat and proteins play major roles. The functional state of the myofibrillar proteins and the content of connective tissue proteins such as collagen and elastin are considered the most important proteins affecting the optical reflectance (Swatland & Barbut, 1990). Meat proteins serve as the natural emulsifying agent in meat emulsion. The most prevalent protein in meat and the most important for fat emulsification and water holding capacity of processed meats is myosin. In addition, fat concentration has a large effect on reflectance measurements at all visible wavelengths (Franke & Solberg, 1971), especially when fat is comminuted together with lean muscle. Light scattering by fat globules and myofibrillar proteins causes meat to appear dark or pale depending on the muscle pH (Swatland, 2002). These two components scatter light differently based

* Corresponding author at: Department of Biosystems and Agricultural Engineering, University of Kentucky, 128 C.E. Barnhart Building, Lexington, KY 40546-0276, USA. Tel.: +1 859 257 3000; fax: +1 859 257 5671.
E-mail addresses: dalvarez@um.es, alvarez.daniel@bae.uky.edu (D. Álvarez).

0963-9969/$ - see front matter © 2010 Elsevier Ltd. All rights reserved.
doi:10.1016/j.foodres.2010.03.002

on their differences in concentration, the number density, and the optical properties (e.g. index of refraction). However, because NIR spectrophotometry is sensitive to fat content, and fat content has many effects on product quality, it may be difficult to extract information that relates directly to protein functionality (Swatland, 2002).

The extinction of a beam of light passing through a scattering medium is governed by the radiative transfer equation (Modest, 2003). In an optically thin medium (less particles and less light scattering) this equation can be reduced to Beer's law:

$$I_f = I_o e^{(-\beta d)} \quad (1)$$

where I_o is the intensity leaving the light source, I_f the intensity reaching the detector, d the distance between the source and detector, and β the light extinction coefficient. According to this equation the light extinction coefficient is used to describe how the original beam of light from the emitting fiber decreases as it travels trough the sample according to absorption and scattering principles. As reported by Crofcheck, Payne, Hicks, Mengüç, and Nokes (2000), the propagation of the light beam can be treated as a planar wave in these optically thin solutions. In this case first-order scattering prevails, meaning that scattering only occurs once before reaching the detector. However, in an optically mixed medium as meat emulsions where the number of particles increase during chopping process, scattering increases and higher order scattering becomes important and Eq. (1) no longer applies.

This study was undertaken to further study the scattering of light in beef meat emulsion and to test the feasibility of using a fiber optic technology to determine whether the apparent light extinction coefficient (β) or fat/nonfat solid (basically meat proteins) concentrations can be used for predicting the normalized intensity of the light signal. An ideal on-line optical system for measuring light scattering in meat emulsion making should basically respond to fat/nonfat solids concentration changes during emulsification, as well as structural or textural changes related to the redistribution of air bubbles in meat matrix.

2. Materials and methods

Data analyzed in this study correspond to the data set presented previously (Álvarez et al., 2009), where details of the materials and methods were presented. Hence, only a brief description of the main aspects of special relevance is provided here.

2.1. Experimental design

A factorial design in set blocks with three batches was performed to gather basic information about the backscatter light extinction properties of beef meat emulsions for the development of an optical sensor technology. Each set block was made in three replications and each batch was performed at a different level of chopping length (CT: 2, 5 and 8 min). For each chopping time selected (batch), three levels of fat/lean ratio (R_{FL}: 0.075, 0.25 and 0.33) were used to determine the effect of chopping process duration and different proportions of fat on technological parameters associated with emulsion stability (i.e., water and fat separation). Three distances (d: 2, 2.5 and 3 mm) between optical delivery and collected fibers were used to determine the light extinction as a function of wavelength. The least square means of chemical composition of raw materials (means of R_{FL}) used to prepare the different batches was not significantly ($P > 0.05$) different. A different batch of meat was assigned to each experimental block. Since block and batch effects were not independent, the three different meat batches were sampled and analyzed for chemical composition to disregard a potential confounding effect between meat batch and the experimental blocks. No significant differences ($P > 0.05$) were found between blocks for the least square means of R_{FL} at any of the three target R_{FL} experimental levels, which discard a batch-block confounding effect.

2.2. Sample preparation and meat emulsion manufacturing

Commercial fresh ground beef samples were obtained from a local meat purveyor (Kroger Co. Cincinnati, OH). Chemical composition (fat and moisture) of each meat batch were measured before processing. The raw materials, with the specific R_{FL}, were weighted and vacuum packed into individual plastics bags and frozen at −18 °C until use. Before emulsion manufacturing, frozen samples were thawed to ~1 °C. Each emulsion was prepared using 100 g of ground beef, 6.35 g of additives (hot dog seasoning RD 105-68A, United Food Ingredients, Inc. Beecher, Illinois, USA) and 26 g of ice. Ground beef samples and ingredients were comminuted in a bowl chopper (KitchenAid, Mod. KFP710, St. Joseph, Michigan, USA) at 1750 rpm for 2, 5 and 8 min (blocks 1, 2 and 3, respectively). Immediately after chopping, temperature of the meat emulsions was measured using a Traceable® Thermometer (Mod. 15-078G. Control Company, Tx., USA).

2.3. Proximate analysis

Chemical composition (fat and moisture, %) of the commercial fresh ground beef samples and raw meat emulsions were analyzed using a HFT-2000 fat analyzer (DSC – Data Support Co. – Inc., Encino, CA, USA; accuracy of ±0.5%). The fat analyzer was previously calibrated and programmed to determine fat and moisture concentration in beef meat. Samples of ~3 g were weighted in a balance Adventure™ (Mod. ARA520, Ohaus® Corp., USA) over a glass fiber pad (Mod. 1019, Data Support Co. Inc., USA). Then, samples were covered with another pad, gently pressed, and placed into the fat analyzer plate for measurement. Samples were measured in triplicate and the average was recorded.

2.4. Light backscatter measurement of raw emulsions

An optical sensor prototype was connected to a High-Resolution Fiber Optic Spectrometer (Model HR4000, Ocean Optics, Inc., Dunedin, FL, USA) by two 600 μm diameter optical fibers (Spectran Specialty Optics, Avon, CN, USA) to measure light backscatter of comminuted meats at different optical path lengths (Fig. 1). This optical measuring device was designed to set the radial distance between the optical emitting and detecting fibers by means of a micrometer, according to previous studies of Payne, Zhou, Sullivan, and Nokes (1997). Infrared light from a light emitting diode (LED) is transmitted to the probe tip through one leg of a bifurcated fiber cable. Light reflected from the meat emulsion matrix particles is transmitted through the receiving fibers to a photodetector. The light source utilized was a tungsten halogen (300–1100 nm) bulb (LS-1, Ocean Optics, Inc.). A PC connected by a USB port to the spectrometer was programmed for data acquisition with SprectraSuit Spectroscopy platform software (Ocean Optics, Inc.). Before each measurement, the terminating ends of the fibers were aligned vertically and horizontally to the same level. Emulsion samples were placed in a double-jacketed sample holder and an opaque enclosure was used to eliminate external light interference. The fiber tips were immersed into the emulsion sample up to a final depth of ~12.7 mm from the surface of the sample. The temperature of the sample was controlled by means of connecting the sample holder to a water bath (Lauda Ecoline RE220. Brinkman Instruments Inc., NY, USA; ±0.01 °C of accuracy) and was ~10 °C in all cases.

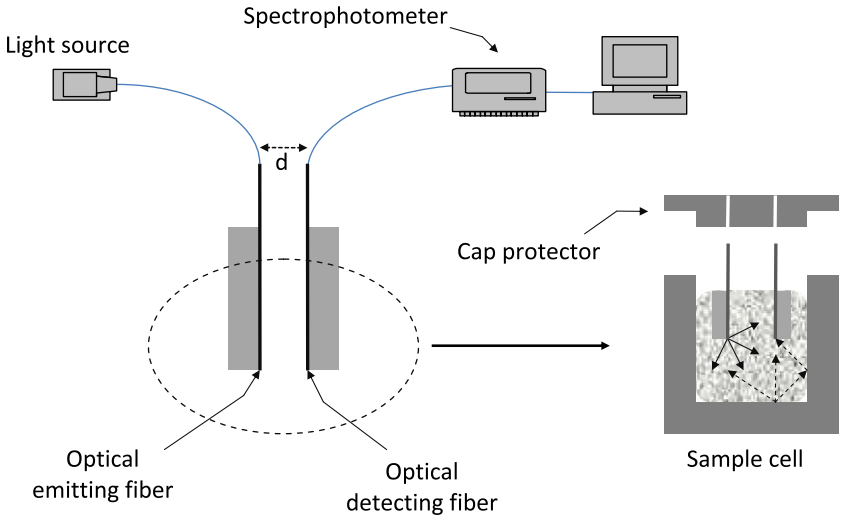

Fig. 1. Schematic diagram of the optical system configured for measuring of light backscatter signal at different radial distances (d = optical fiber separation from 2 to 3 mm) from the light source, using a fiber optic cable of 0.6 mm diameter.

2.5. Data analysis and calculation of normalized spectral scans

Light backscatter intensity of the samples was measured at the target radial distances according to the experiment design described in Section 2.1., and at an integration time (*IT*) ranging from 19 to 60 s, where *IT* was the detector light exposure time. The light scattering spectral data was analyzed to determine whether the apparent light extinction coefficient (β) and the concentrations of fat and nonfat solids could be used to predict the normalized intensity of the optical signal. The light scattering spectral scans, $I(\lambda)$ was automatically processed by subtracting the respective dark spectral scans for light scattering and dividing by the *IT* to give the normalized spectral scans for light scattering, $I_N(\lambda)$ (bits s^{-1}). The light scattering profiles as a function of fat/lean ratio were calculated by reducing each normalized spectral scan, $I(\lambda)$, to 18 averages by dividing them into 30 nm wavebands with mid-wavebands of $485 + 30n$ ($1 \leqslant n \leqslant 18$) and averaging the optical scattering response for the wavelengths constituting each waveband. The 18 wavebands obtained were in the range 500–1010 nm. Following the prediction models established by Crofcheck et al. (2000) and Castillo, Payne, López, Ferrandini, and Laencina (2005) to predict milk fat content in skim milk and whey fat concentration in cheese making, respectively, we suggest the following two models to predict the normalized intensity (I_{N_0}) of the optical signal leaving the light source during meat emulsification, considering that scattering light distribution is dominant:

$$I_N = I_{N_0} \exp(-\beta d)/d^2 \quad (2)$$

$$I_N = I_{N_0} \exp(-(afat + bN_{FS})d)/d^2 \quad (3)$$

where I_{N_0} is the normalized intensity leaving the light source, d is the distance between optical fibers (mm) and β is the apparent light extinction coefficient (mm^{-1}). This coefficient is defined as $\beta = \alpha c$, where α is the light extinction coefficient and c is the concentration value of the parameter fat/lean ratio. In Eq. (2), c is constant and consequently $\beta = \alpha$, while in Eq. (3), a and b were constants and β coefficient was considered as a function of fat and nonfat solid (N_{FS}) concentrations (the terms "*a fat*" and "*b* N_{FS}" are expressed in mm^{-1}). As can be observed, both equations are developed under a specific distance (d) between emitting and detecting optical fibers. In order to determine the effect of the parameter distance on the changes of light extinction coefficients for prediction, we have included a second distance in the Eq. (2) and studied the intensity ratios as follows:

$$\frac{I_1}{I_2} = \frac{I_0 e^{-\alpha c d_1/d_1^2}}{I_0 e^{-\alpha c d_2/d_2^2}}$$

This equation can be simplified as follows:

$$\frac{I_1}{I_2} = \left(\frac{d_2^2}{d_1^2}\right)\frac{e^{-\alpha c d_1}}{e^{-\alpha c d_2}} = c_1 e^{+\alpha c(d_2 - d_1)}$$

where c_1 is the square ratio between distance d_2 (2.5 mm) and distance d_1 (2 mm). Solving this intensity ratio we obtain this equation:

$$\ln\left(\frac{I_1}{I_2}\right) = \ln c_1 + \alpha c(d_2 - d_1) = \beta_0 + \beta_1(d_2 - d_1)$$

where β_0 is the parameter of geometry and it is defined as $\beta_0 = \ln c_1$, and β_1 is the extinction parameter defined as $\beta_1 = \alpha c$. Finally, this equation yields the next prediction model:

$$\beta_1 = \left[\ln\left(\frac{I_1}{I_2}\right) - \beta_0\right]/(d_2 - d_1) \quad (4)$$

All the light scattering spectral data was simultaneously tested using the software tool Excel Solver to determine the apparent light scattering and the fat/nonfat solid concentrations for prediction of normalized intensity (I_{N_0}) using model I (Eq. (2)), model II (Eq. (3)) and model III (Eq. (4)).

3. Results and discussion

3.1. Effect of fat/lean ratio on normalized backscatter spectral scan

Fig. 2 shows the typical normalized backscatter spectral scan as a function of fat lean ratio. As can be observed, backscatter response intensity was inversely proportional to fat lean ratio, especially in the central spectral scan corresponding to the orange–red (610–640 nm) and red (670–700 nm) regions where I_N showed a clear decrease as R_{FL} increased from 0.075 to 0.33. Crofcheck et al. (2000) observed a similar behavior of the normalized intensity at 724 nm in milk samples with various fat levels. However, when the change of I_N is studied as a function of R_{FL} (Fig. 3) this behavior changes accordingly with the changes of the spectral scan and chopping time analyzed. As can be observed in the Fig. 3, I_N increases as R_{FL} of samples increases from 0.075 to 0.25, declining after this point until $R_{FL} = 0.33$. This behavior is observed at spectral scans up to 620 nm and CT of 2 and 5 min, but an opposite

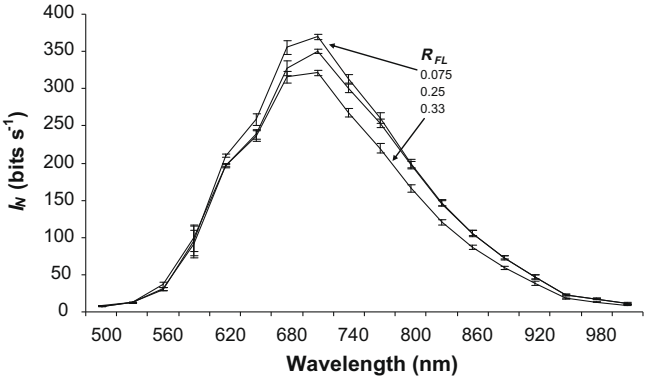

Fig. 2. Typical normalized intensity (I_{N1}) spectral scan (5 min CT, 2 mm between optical fibers) as a function of fat/lean ratio (R_{FL}). Error bar corresponded to standard deviation interval of 18 average values of I_N, divided into 30 nm waveband (485 nm–1025 nm). For each interval of I_N, N = 117.

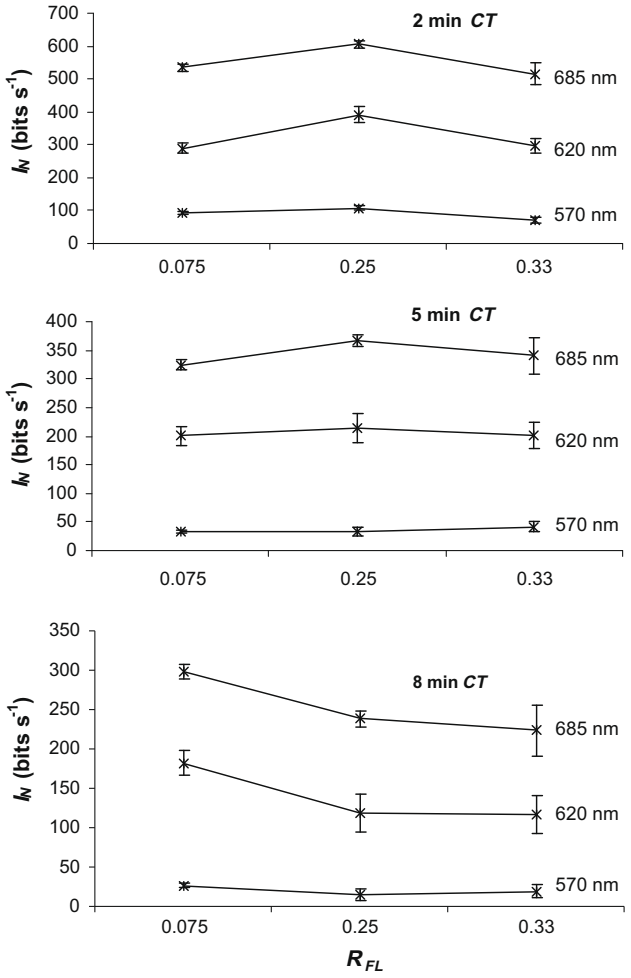

Fig. 3. Evolution of the normalized intensity (I_{N1}) as a function of fat/lean ratio (R_{FL}), at each spectral scan and chopping time analyzed.

behavior of I_N is detected at 570 nm and 8 min of CT. These results suggest that I_N is able to pass easily throw the samples with short or moderate chopping lengths until a critical point of fat concentration (R_{FL} = 0.25). After this point, light backscatter decreases as fat concentration and CT increase. This trend in the I_N suggests that light scattering intensity is not only proportional to particle concentration but also depends on the reduction of particle size that is reached as CT increase. According to previous studies (Modest, 2003; Pizzino, Catté, Van Hecke, Salager, & Aubry, 2009) light scattering intensity is not only proportional to particle concentration but also depends, among other properties, on the material of the particle (i.e., the complex index of refraction) and its size parameter ($\pi d/\lambda$, where d is the diameter of the particle). This decrease in the intensity signal and consequently higher light scattering as particle size decrease was also observed in previous studies of the increase in aggregate size of protein gels formed by gradually increasing Na concentration (Barbut, 1996). This author observed that the increase in aggregate size not only increases the opacity of the gels (low scattering of light) but also resulted in larger open spaces within the gel structure which caused a reduction in capillary forces and hence WHC (water holding capacity). Similar results were obtained by Hermansson (1988) in gel structure of food biopolymers. However, for other authors the reduction in particle size caused by chopping during emulsion formation has little optical effect (Swatland, 2002), but this reduction in particle size allows the inclusion of air bubbles in the meat matrix, increasing light scattering and the product paleness (Palombo, Van Roon, Prins, Koolmees, & Krol, 1994). Otherwise, if batters are stored or if there is a redistribution of air from small to larger bubbles, scattering tends is to decrease (Swatland, 2002).

3.2. Prediction of normalized intensity

All the possible combinations between dependent (fat and nonfat solids concentrations) and independent (spectral scan, chopping time and fat/lean ratio) variables included in both models I (27 combinations with N = 9 each) and II (nine combinations with N = 27 each) were analyzed using Eqs. (2) and (3) to establish the best model for predicting I_{N_0} signals. Tables 1 and 2 show the six combinations of independent variables yielding the highest R^2 using model I (Eq. (2)) and model II (Eq. (3)), respectively. The R^2 values were within a high range in each model (0.978–0.992 for model I, and 0.931–0.973 for model II) suggesting that the models and their six best combinations had a different predictive ability. These data show that model I, where fat and lean concentrations

Table 1
The six combinations of wavelength, chopping time (CT) and fat lean ratio (R_{FL}) yielding the highest R^2 using model I (Eq. (2)) for predictions*.

Order	Wavelength (nm)	CT (min)	R_{FL}	I_{N_0}	β	R^2
1	570.17	8	0.075	6.177	8.828	0.992
2	570.17	2	0.075	53.01	13.26	0.988
3	685.13	8	0.075	11.58	−0.118	0.986
4	625.15	8	0.25	10.64	4.099	0.986
5	685.13	8	0.25	10.09	0.325	0.985
6	685.13	5	0.25	15.92	0.463	0.980

* For each regression, N = 9. I_{N_0}; normalized intensity leaving the light source. β; apparent light extinction coefficient (mm^{-1}).

Table 2
The six combinations of wavelength and chopping time (CT) yielding the highest R^2 using model II (Eq. (3)) for predictions*.

Order	Wavelength (nm)	CT (min)	I_{N_0}	*Fat*	N_{FS}	R^2
1	625.15	8	17.28	0.217	0.163	0.973
2	685.13	8	14.85	0.114	0.031	0.956
3	685.13	5	17.59	−0.02	0.074	0.950
4	625.15	5	21.56	0.032	0.222	0.946
5	570.17	8	5.927	0.252	0.357	0.936
6	685.13	2	29.63	0.017	0.062	0.931

* For each regression, N = 27. I_{N_0}; normalized intensity leaving the light source. N_{FS}, nonfat solids (mm^{-1}).

are constant, is significantly ($P < 0.0001$) better than model II, where the apparent light extinction coefficient is considered in function of fat and N_{FS} concentrations, to predict the normalized intensity of light backscatter signal. No significant difference ($P > 0.05$) was found between the least square means of the I_{N_0} predictions obtained by model I and II. The best combinations of independent variables to predict the normalized intensity were 570 nm of wavelength (λ), 8 min CT and 0.075 R_{FL} for model I, and 625 nm, 8 min CT for model II. The results suggest that increase of fat sample were associated with the largest I_{N_0} prediction errors (model I), observing the three best predictions with the lower fat values. Both models also showed the best predictions as CT increase from 5 to 8 min, observing the most frequent value of CT at 8 min. The wavelength (λ) analyzed in both models showed inconclusive results. In model I the best predictions are observed in the green–yellow spectral scan (555–585 nm) while in model II these predictions are observed in the orange–red (610–640 nm) and red (670–700 nm) spectral scans.

3.2.1. Effect of particle size and fat/lean concentration on I_{N_0} prediction

Figs. 4 and 5 show the best prediction of I_{N_0} for models I and II using light extinction coefficient (Eq. (2)) and the concentrations of fat and nonfat solids (Eq. (3)), respectively. As can be observed, model I had a larger R^2 (0.99) than model II (0.97), but the coefficient of variation (CV) was less in model II (0.75) than I (4.88). From this model II, it follows that the response of orange–red light (610–700 nm) and longer chopping times (CT = 8 min) for I_{N_0} prediction was proportionally higher than the response of the green–yellow light (555–585 nm) and short chopping times (CT = 2 min). The observed pattern is considered to be related to the fat/lean concentration and particle size reduction during emulsification process, and can be also observed in the evolution of I_N previously described in the Fig. 3. In this figure, light scattering signal increases as R_{FL} increases in emulsions made with low fat/lean ratio (from 0.075 to 0.25) and chopping time (2 and 5 min). In those conditions, the most important effect over the optical parameters is considered to be related with the low concentration of particles, as a result of the short chopping conditions. However, at CT = 8 min the light scattering signal is proportional to the particle size, observing a linear decrease of I_N at low R_{FL} (from 0.075 to 0.25). In these conditions, light intensity signal shows high difficulty to pass throws the sample when meat emulsion is highly chopped and particle size decrease. Otherwise, at high R_{FL} (from 0.25 to 0.33) light scattering signal is linearly proportional to concentration, observing a decrease of I_N for each chopping duration

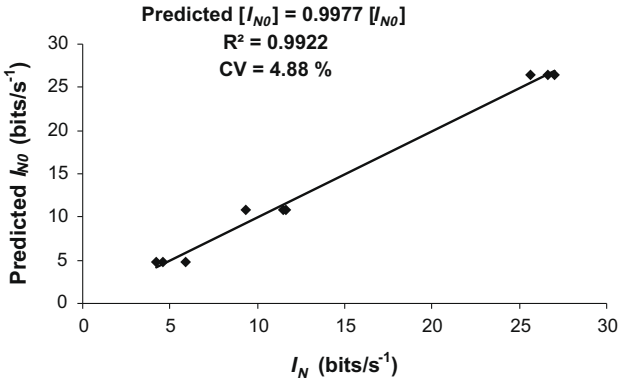

Fig. 4. Prediction of light backscatter normalized intensity (I_{N_0}; at $d = 0$) as a function of the normalized intensity (I_N; at $d = 2$, 2.5 and 3 mm) and a constant concentration of fat and lean ($R_{FL} = 0.075$), using model I (Eq. (2)). For prediction were used the regression coefficient, $\beta = 8.828$, and the independent variables CT = 8 min and 570.17 nm of spectral scan. $N = 9$. d = distance between optical fibres.

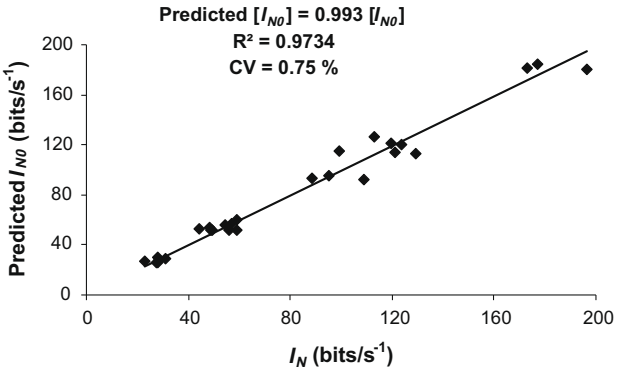

Fig. 5. Prediction of light backscatter normalized intensity (I_{N_0}; at $d = 0$) as a function of the normalized intensity (I_N; at $d = 2$, 2.5 and 3 mm), using model II (Eq. (3)). For prediction were used the regression coefficient, *fat* (R_{FL}) = 0.2173, *nonfat solids* (N_{FS}) = 0.1627, and the independent variables, CT = 8 min and 625.15 nm of spectral scan. $N = 27$. d = distance between optical fibres.

(from 2 to 8 min), independently of the particle size of the sample obtained after chopping. Experimental evidences with suspension of particles of different size in the 0.1–20 μm range support that light backscatter passes through a maximum for a size about 0.5 μm (saturation point), declining after this point even throw the particle size increases (Buron, Mengual, Meunier, Cayré, & Snabre, 2004). Similar behavior of light scattering was observed by Castillo et al. (2005) using a fiber optic technology to predict whey fat concentration. These authors observed that light scattering was linear with a low fat concentration of milk samples but as fat increases a point of saturation was reached and the intensity no longer holds, declining even though the concentration increases. This behavior described for the authors is observed in our results at 2 and 5 min of CT where the particle proportion of moderate size is high, but it is not observed at 8 min CT where the reduction of particle size highly influences the light transmission throw the meat sample. These results suggest that light scattering of meat emulsion samples shows a great variability during chopping process, being highly influenced by the concentration and particle size of samples.

3.2.2. Effect of spectral scan on I_{N_0} prediction

Fig. 3 also shows the evolution of I_N as a function of the spectral scan analyzed. As can be observed, a linear increase of I_N is detected as spectral scan increases from 570 to 685 nm in all the chopping conditions. Fig. 3 also shows a point of light intensity saturation at 620 and 685 nm in emulsions made with 0.25 of R_{FL} and moderate chopping durations (2–5 min) that is not observed at 570 nm of spectral scan, as well as in emulsions made during 8 min of CT. This behavior suggests a highly dependent correlation between functional properties of meat emulsions, such as fat/lean proportion, and specific peaks of the spectral scan. According to Swatland (2002), in meat mixtures, lipid content is the major variable in these correlations and the strongest relationships are obtained with red or near infrared (NIR). But if variation in lipid content is cancelled so that pH-dependent protein properties are dominant, then the peak correlations are with shorter wavelengths. As a result, we hypothesized that the best combination showed in Table 1 yielding the highest R^2 (model I, Eq. (2)) at lower spectral scan (520.17 nm) and fat/lean ratio (0.075) could be correlated with higher proportion of lean proteins in these emulsions, while increasing the proportion of fat (0.25 R_{FL}), the best predictions are observed at higher spectral scan (685 nm). These peak correlations are highly wavelength dependent and apparently contain information of functional properties that could be used to estimate normalized intensity of light backscatter signal.

3.3. Light extinction coefficients for prediction

Light extinction coefficients for I_{N_0} prediction have been previously described using two models under a specific optical distance between fibers, and a model where light extinction coefficient is considered in function of the intensity ratio obtained between two optical distances. In model I (Eq. (2)) the apparent light extinction coefficient (β) is used under a constant concentration value ($\beta = \alpha$) (mm^{-1}), while in the model II (Eq. (3)) the concentration is considered in function of fat/nonfat solids (N_{FS}) values (mm^{-1}). In model III (Eq. (4), light backscatter intensity obtained using two distances between fibers is considered to determine light scattering coefficient for prediction.

3.3.1. Models based on a specific distance between optical fibers

Fig. 6 shows the polynomial regression of the apparent light extinction coefficient (β) as a function of wavelength, in the range of 550–700 nm. This light extinction coefficient showed a high range between the maximum value $\beta = 13.26$ (mm^{-1}) located a 570 nm (green–yellow spectral scan) and the minimum value $\beta = -0.90$ (mm^{-1}) located in the NIR spectral scan (685 nm). Fig. 7 shows the polynomial regression of nonfat solids (N_{FS}) as a function of the wavelength, in the same spectral scan waveband. This parameter showed a tight range between the maximum value $N_{FS} = 0.508$ mm^{-1} at 570 nm and the minimum value $N_{FS} = 0.031$ mm^{-1} at 685 nm. According with the best predictions for I_N detected in Tables 1 and 2 using models I and II, respectively, these results suggest that the best prediction of I_{N_0} using the apparent light extinction (Fig. 6) is detected at the green–yellow spectral scan (570 nm) when the samples has a low fat lean ratio (Table 1) and their lean protein proportion is dominant. Otherwise, when the fat lean ratio is considered in the equation (Eq. (3), Model II) the best predictions of I_N detected in the orange-red (625 nm) or NIR spectral scan (685 nm) (Table 2) are observed as N_{FS} decrease (Fig. 7). This behavior coincides with those described by Williams and Norris (1987) where any medium that is absorbing light, the decrease in intensity I per unit length d is proportional to the medium concentration as a result of multiple scattering. In these conditions, light interacts with several particles, especially fat and proteins, and travels for longer distances in the medium. Thus, as can be observed in the Fig. 7, the multiple scattering effects are less pronounced when the light absorption by fat particles is higher (lower minimum value N_{FS} at 685.13 nm). These results show that the use of optical wavebands for the study of the light backscatter extinction in finely comminuted meat emulsions may have potential for predicting the normalized intensity in a wide spectral scan range (500–700 nm).

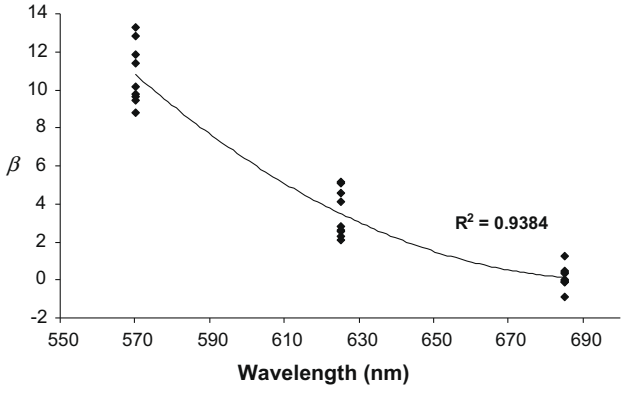

Fig. 6. Plot representation of apparent light extinction coefficient (β; mm^{-1}) as a function of wavelength (nm), fitted to model I (Eq. (2)).

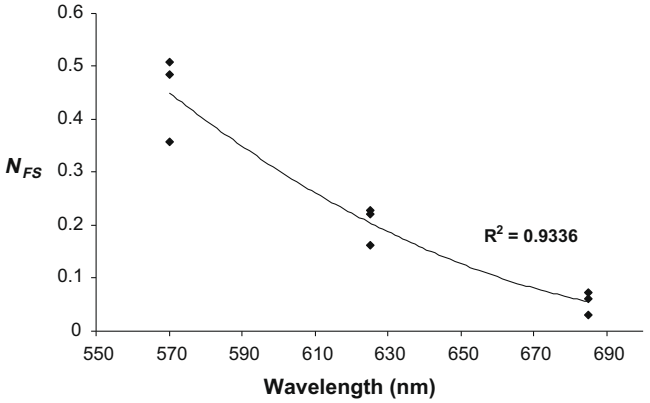

Fig. 7. Plot representation of nonfat solids (N_{FS}, mm^{-1}) as a function of wavelength (nm), fitted to model II (Eq. (3)).

Table 3
Values of the geometry and extinction coefficients obtained at different distances between optical fibers and the R^2 values of β_1 (mm^{-1}) as a function of fat/lean ratio (R_{FL}), spectral scan and chopping time (CT) parameters used for prediction of normalized intensity using the model III (Eq. (4))*.

Ratio intensity	Distance difference (mm)	Geometry coefficient (β_0)	Extinction coefficient (β_1)	R^2		
				β_1 *vs* R_{FL}	β_1 *vs* *Scan*	β_1 *vs* CT
I_1/I_2	0.5	0.446	0.548	0.709	0.689	0.004
I_2/I_3	0.5	0.365	0.678	0.444	0.454	0.050
I_1/I_3	1	0.811	0.613	0.760	0.755	0.008

* $N = 81$.

3.3.2. Models based on light intensity ratio of two optical distances

Table 3 shows the values of the geometry and extinction coefficients, as well as the R^2 values of β_1, using the model III (Eq. (4)). As can be observed, the increase of distance between optical fibers is associated with increases of the geometry (β_0) and extinction (β_1) coefficients. The light extinction is maximum (0.678 mm^{-1}) between optical distances 2.5 and 3 mm, where a lower light intensity is reached by the detecting fiber, indicating that light absorption increases with radial distance. This increase of light extinction is maximum at high distance between fibers (1 mm), yielding the higher R^2 as fat lean ratio of the samples (0.760) and spectral scan analyzed (0.755) increases. These results are in agreement with those obtained with the previous models I and II, indicating that high fat level of samples and spectral scans (orange–red and red wavebands) are the parameters studied with higher light scattering.

4. Conclusions

The behavior of normalized light backscatter response as a function of fat/lean ratio, chopping time and wavelength was studied using different models. Model I, where fat/lean concentration is constant and light scattering distribution is dominant, was significantly ($P < 0.0001$) better than model II (light extinction coefficient is considered in function of fat and nonfat solids (N_{FS}) concentrations) for prediction of normalized light backscatter signal (I_{N_0}). This intensity prediction was estimated with a R^2 of 0.99 and a CV of 4.88% using model I with a chopping duration of 8 min and a short waveband of 570 nm. Light scattering intensity showed a linear correlation with particle concentration as well as the reduction of particle size as chopping time increased (model II). Light extinction was maximum at high distance between optical fibers (model III), yielding the higher R^2 as fat lean ratio of the samples (0.760) and spectral scan analyzed (0.755) increases. These results

suggest a high correlation between functional properties of meat emulsion (i.e., fat/lean proportion) and specific peaks of the spectral scan. These wavelength correlations apparently contain information of functional properties that could be used in finely comminuted meat emulsions for predicting the normalized intensity of light backscatter signal in a wide spectral scan range (500–700 nm).

Acknowledgements

The authors wish to thank the Séneca Foundation (Consejería de Educación y Cultura. CC.AA. Murcia, Spain) and the Kentucky Science and Engineering Foundation (University of Kentucky, USA) for the financial support provided by the research projects "Applying optical sensor technologies for determining meat emulsion stability" and "Development of an optical backscatter sensor technology for monitoring and controlling meat emulsification during the chopping process".

References

Álvarez, D., Castillo, M., Payne, F. A., & Xiong, Y. L. (2009). A novel light backscatter fibre optic sensor for monitoring stability during beef meat emulsification. *Meat Science, 81*, 456–466.

Barbut, S. (1996). Use of fibre optics to study the transition from clear to opaque whey protein gels. *Food Research International, 5–6*, 465–469.

Buron, H., Mengual, O., Meunier, G., Cayré, I., & Snabre, P. (2004). Review optical characterization of concentrated dispersions: applications to laboratory analyses and on-line process monitoring and control. *Polymer International, 53*, 1205–1209.

Castillo, M., Payne, F. A., López, M. B., Ferrandini, E., & Laencina, J. (2005). Optical sensor technology for measuring whey fat concentration in cheese making. *Journal of Food Engineering, 71*, 354–360.

Crofcheck, C. L., Payne, F. A., Hicks, C. L., Mengüç, M. P., & Nokes, S. E. (2000). Fibre optic sensor response to low levels of fat in skim milk. *Journal of Food Process Engineering, 23*, 163–175.

Franke, W. C., & Solberg, M. (1971). Quantitative determination of metmyoglobin and total pigment in an intact meat sample using reflectance spectrophotometry. *Journal of Food Science, 36*, 515–519.

Hermansson, A. M. (1988). Gel structure of food biopolymers. In J. M. V. Blanshard & J. R. Mitchell (Eds.), *Food structure, its creation and evaluation*. London: Butterworths.

Krol, B., van Roon, P. S., & Houben, J. H. (1988). *Trend in modern technology 2*. Wageningen: Pudoc.

Lanza, E. (1983). Determination of moisture, protein, fat and calories in raw pork and beef by near infrared spectroscopy. *Journal of Food Science, 48*, 471–474.

Modest, M. F. (2003). *Radiative heat transfer*. Massachusetts: Academic Press.

Norris, K. H. (1984). Reflectance spectroscopy. In K. K. Stewark & J. R. Whitaker (Eds.), *Modern methods of food analysis*. Westport, CT: AVI Publishing Company.

Palombo, R., Van Roon, P. S., Prins, A., Koolmees, P. A., & Krol, B. (1994). Changes in lightness of porcine lean meat batters during processing. *Meat Science, 38*, 453–476.

Payne, F. A., Zhou, Y., Sullivan, R. C., Nokes, S. (1997). Radial backscatter profiles in milk in the wavelength range of 400 to 1000 nm. ASAE Meeting Presentation. Paper No. 976097. St. Joseph, MI, USA.

Pizzino, A., Catté, M., Van Hecke, V., Salager, J.-L., & Aubry, J.-M. (2009). On-line light backscattering tracking of the transitional phase inversion of emulsions. *Colloids and Surfaces A: Physicochemical and engineering aspects, 338*, 148–154.

Swatland, H. J. (1982). Fiber optic spectrophotometry and the wetness of meat. *Journal of Food Science, 47*, 1940–1942.

Swatland, H. J. (1983). Infrared fiber optic spectrophotometry of meat. *Journal of Animal Science, 56*, 1329–1333.

Swatland, H. J. (2002). On-line monitoring of meat quality. In J. Kerry, J. Kerry, & D. Ledward (Eds.), *Meat processing improving quality* (pp. 193–216). Woodhead Publishing.

Swatland, H. J., & Barbut, S. (1990). Fibre-optic spectrophotometry for predicting lipid content, pH and processing loss of comminuted meat slurry. *International Journal of Food Science and Technology, 25*, 519–526.

Williams, P., Norris, K. (1987). *Near-infrared technology in the agricultural and food industries*. St. Paul, Minnesota, USA: The American Association of Cereal Chemists, Inc.